Characterization of Poly(amidoamine) Dendrimers and Their Complexes with Cu^{2+} by Matrix-Assisted Laser Desorption Ionization Mass Spectrometry

Li Zhou, David H. Russell,* Mingqi Zhao, and Richard M. Crooks*

Department of Chemistry, Texas A&M University, P.O. Box 30012, College Station, Texas 77842-3012

Received October 16, 2000; Revised Manuscript Received February 20, 2001

ABSTRACT: Hydroxyl-terminated poly(amidoamine) (PAMAM) dendrimers of generation 2−4 (G*n*-OH, $n = 2$, 3, and 4; $M_r \sim 3.7$, 6.9, and 14.3 kDa, respectively) and dendrimers encapsulating Cu^{2+} ions have been investigated by matrix-assisted laser desorption ionization time-of-flight (MALDI-TOF) mass spectrometry. Umbelliferone (7-hydroxycoumarin) and 2′,4′,6′-trihydroxyacetophenone (THAP) were used as the matrices for dendrimers with and without Cu^{2+} in the interior. The MALDI-TOF results provide accurate molecular weight determinations of all dendrimers and some multiple copper complexes of G2-OH and G3-OH (accuracy <0.01%). More importantly, this approach provides direct characterization of multiple-cation adducts and quantitative evaluation of the complexing capacity of dendrimers hosting transition-metal ions. The results are used to determine dendrimer structure and evaluate polydispersity.

Introduction

Here, we report a detailed analysis of hydroxyl-terminated poly(amidoamine) (PAMAM) dendrimers (G*n*-OH) and their complexes with Cu^{2+} using matrix-assisted laser desorption ionization time-of-flight (MALDI-TOF) mass spectrometry (MS) and UV−vis spectroscopy. The results indicate that both complete dendrimers and dendrimers containing serial defects are present in second (G2)-, third (G3)-, and fourth (G4)-generation PAMAM dendrimers. The data also indicate that Cu^{2+} partitions into dendrimers from aqueous solution and that the maximum number of ions associated with each dendrimer increases exponentially with increasing dendrimer generation.

Dendrimers[1,2] possess some desirable chemical and structural characteristic that make them well-suited for a variety of technological applications including drug delivery,[3] gene therapy,[4,5] chemical sensing,[6,7] and catalysis.[8−12] For example, higher generation PAMAM dendrimers are large (∼10 nm in diameter for G8), are globular in shape, and have void spaces within their interiors that can host molecular,[13] ionic,[9,10,14−18] or nanoparticulate[9,10,18] guests (Scheme 1). It is also a straightforward matter to functionalize the exterior of most dendrimers, including the PAMAM family used in this study, and thus control many of their chemical properties including solubility.[1,2,11,19,20] Because of their potential economic significance, there is great deal of interest in developing a detailed understanding of the chemical and structural properties of dendrimers, especially those that are commercially available at the present time.

We previously reported that many different transition metal ions, including Cu^{2+}, Pd^{2+}, Pt^{2+}, Ru^{3+}, and Ni^{2+}, extract into the interior of G*n*-OH dendrimers from solution (Scheme 1)[9,10,18] and that the average number of metal ions within each dendrimer is determined by the relative concentrations of the dendrimer and metal ions, the size of the dendrimer, and the type of metal ion. Dendrimer encapsulation of metal ions is generally driven by a strong association between the ion and intradendrimer tertiary amine groups. Chemical reduction of dendrimer-encapsulated metal ions yields soluble dendrimer-encapsulated metal nanoparticles that usually contain the same number of atoms as were preloaded into the dendrimer "template" initially. Accordingly, control over the number of metal ions preloaded into the dendrimer template prior to reduction is critical for the synthesis of well-defined nanoclusters, which are of fundamental scientific importance and may have significant technological applications.[21−24] To understand the relationship between dendrimer structure, dendrimer complexes with metal ions, and dendrimer-encapsulated nanoparticles, it is important to fully characterize the properties of native dendrimers and the corresponding metal-ion complexes.

A number of analytical methods have been used to elucidate the currently accepted structural model for PAMAM dendrimers. These include size-exclusion chromatography,[25] capillary electrophoresis,[26] and NMR.[27] Electrospray ionization mass spectrometry (ESI-MS) has been one of the principal methods used for characterizing the structure and polydispersity of PAMAM,[28,29] poly(propyleneimine),[30−32] and other types of dendrimers.[33] For example, G1−G10 PAMAM dendrimers have been investigated by ESI-MS coupled with Fourier transform ion cyclotron resonance (FT-ICR), and precise mass values were achieved for G4 and lower generation materials by deconvolution of peaks arising from multiply charged ions with m/z value less than 2000.[34] MALDI-TOF spectra exhibit mostly singly charged species, and it is especially useful for characterizing biological molecules because of its high mass range, sensitivity, and accuracy.[35,36] Biological molecules and other polymers carrying metal ions can also be characterized by MALDI-TOF MS, because the composite materials can form singly charged species by losing protons to compensate the metal-ion charge.[37] MALDI has been shown to be an attractive approach for the

* To whom correspondence should be addressed. D. H. Russell: tel 979-845-3345; fax 979-845-9485; e-mail russell@mail.chem.tamu.edu. R. M. Crooks: tel 979-845-5629; fax 979-845-1399; e-mail crooks@tamu.edu.

10.1021/ma001782j CCC: $20.00
Published on Web 03/29/2001

Scheme 1

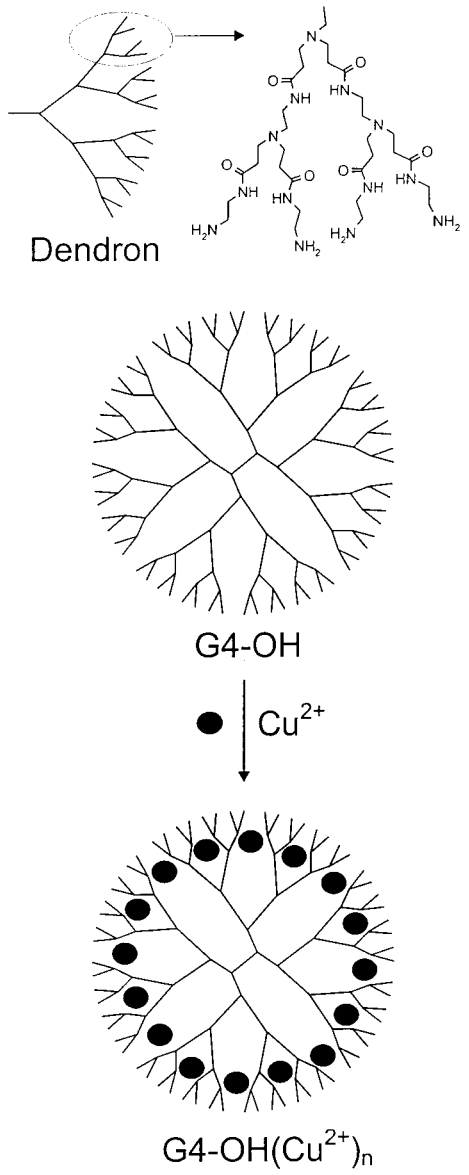

characterization of some dendritic polymers, including those based on polyethers,[38,39] polypyridines,[40] carbosilanes,[41,42] phenylacetylenes,[43] isophthalate ester-terminated polyethers,[44] and other families of dendrimers.[45−50]

In this paper we discuss the polydispersity and structural characteristics of second-, third-, and fourth-generation PAMAM dendrimers (G*n*-OH, $n = 2$, 3, and 4, respectively) and their complexes with Cu^{2+} using MALDI-TOF MS. We also investigated the relationship between the number of extracted Cu^{2+} ions and the generation of the host dendrimers using MALDI-TOF and UV−vis absorption spectroscopy. The results indicate that hydroxyl-terminated PAMAM dendrimers bind Cu^{2+} ions within their interior and that the maximum number of the extracted metal ions increases exponentially as a function of dendrimer generation.

Experimental Section

Chemicals. Hydroxyl- and amine-terminated integral-generation PAMAM dendrimers having an ethylenediamine core were provided as 10−25% methanol solutions (Dendritech, Inc., Midland, MI). Prior to use, methanol was removed by vacuum evaporation at 20 ± 2 °C. $Cu(NO_3)_2 \cdot 2.5H_2O$ (Acros Organics, Pittsburgh, PA) was of reagent quality and used as received. All solutions were prepared with 18 MΩ·cm deionized water (Millipore, Bedford, MA).

For the spectrophotometric titrations, unbuffered (pH ∼ 5.3) 20 mM aqueous $Cu(NO_3)_2$ solutions were used to titrate the unbuffered (pH ∼ 8.1) 0.2 mM G2-OH, 0.1 mM G3-OH, and 0.05 mM G4-OH aqueous dendrimer solutions. The temperature was 20 ± 2 °C during the UV−vis experiments.

Characterization. Absorption spectra were recorded on a Hewlett-Packard HP 8453 UV−vis spectrometer. The optical path length was 1.0 cm, and deionized water was used as reference for all measurements.

The positive-ion MALDI-TOF mass spectra were recorded on a PerSeptive Biosystem Voyager Elite XL TOF mass spectrometer operating in reflectron or linear mode with delayed extraction. The reflectron mode enables isotopic resolution for compounds having a molecular weight under 5000.[35] In the linear mode, peaks are assigned on the basis of average mass values. In both modes, ions were generated by a pulsed nitrogen laser emitting at 337 nm, and 200 laser shots were averaged for each spectrum. The ion source voltage and delayed extraction time were tuned to give good mass resolution over a broad mass range.[51] For example, in reflectron mode, an acceleration voltage of 25 kV was utilized with a grid voltage of 17.5 kV and a delay time of 200 ns. In the linear mode, an acceleration voltage of 25 kV was used with a grid voltage of 22.75 kV and a 200 ns delay time for G2-OH and a 300 ns delay for G3-OH and G4-OH.

Sample Preparation for MALDI-TOF MS. The success of the MALDI experiment is highly dependent on the selection of an appropriate matrix, especially in the case of higher generation dendrimers. Matrixes widely used to analyze peptides and proteins, such as derivatives of cinnamic acid, work well for G2-OH, but protons compete with metal ions for dendrimer binding sites (interior tertiary amines).[18] Also, there is a competition between analytes and matrixes in binding with metal ions.[52] All of these problems make carboxylic acid matrixes inappropriate for analyzing dendrimer−metal ion complexes. Accordingly, we tested a variety of other potential matrixes to optimize ionization and minimize spectral biases induced by proton competition. Umbelliferone and 2′,4′,6′-trihydroxyacetophenone (THAP) were found to yield the best results. The former was used as the matrix for G2-OH and the latter for G3-OH and G4-OH.

Umbelliferone and THAP (Sigma) were used as received to prepare 0.1 and 0.2 M methanolic solutions, respectively. Stock solutions of the dendrimers were diluted to 0.05 mM (G2-OH) or 0.1 mM (G3-OH and G4-OH). The matrix and dendrimer solutions were mixed in a 3:4 ratio, leading to a matrix-to-analyte ratio of 1500:1. MALDI-TOF samples were prepared using the overlayer method.[35,53] First, the concentrated, methanolic matrix solution was deposited onto a stainless steel sample stage. Following rapid evaporation of methanol, 1 μL of the mixed dendrimer/matrix solution was deposited onto the solid matrix and allowed to dry in air. The sample spot was then washed with water (1−2 μL) to remove alkali metal salts, and the water was removed by shaking and allowed to air-dry.[52] This treatment may remove some portion of highly soluble and low molecular weight impurities, but the larger, more hydrophobic analytes remain in the sample spot.

The measured molecular weights were based on a two-point external mass calibration using substance P-amide ($[M + H]^+ = 1348.66$) and oxidized insulin B chain ($[M + H]^+ = 3496.96$) for G2-OH, oxidized insulin B chain and ubiquitin ($[M + H]^+ = 8565.81$) for G3-OH, and horse-heart myoglobin ($[M + 2H]^{2+} = 8476.78$, $[M + H]^+ = 16952.56$) for G4-OH.[35,51] All the mass values listed above refer to the average molecular weights.

Results and Discussion

Metal-Ion-Free Dendrimers. We first investigated the average molecular weights and polydispersity of metal-ion-free PAMAM dendrimers.[54,55] An isotopically resolved mass spectrum of G2-OH is shown in Figure 1a, and observed and calculated mass values are sum-

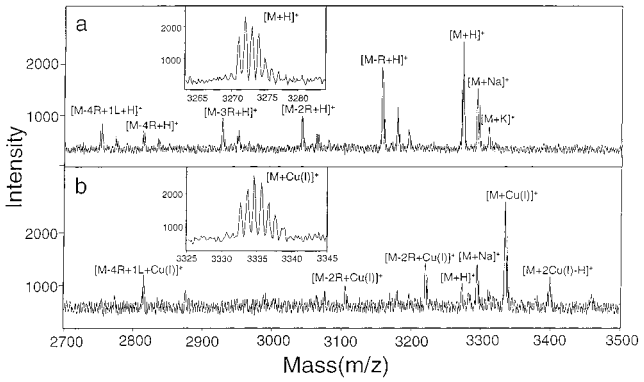

Figure 1. MALDI-reflectron TOF mass spectra of G2-OH in the (a) absence and (b) presence of a 4-fold molar excess of Cu^{2+}. Matrix: umbelliferone. The insets show the expanded isotopically resolved $[G2\text{-}OH + H]^+$ and $[G2\text{-}OH + Cu^+]^+$ peaks. The spectra contain signals arising from the loss of the R group ($R = -CH_2CH_2CONHCH_2CH_2OH$, −115 Da) and formation of intramolecular loops (L, −60 Da) after loss of four R groups. M represents a PAMAM dendrimer having an ideal, defect-free structure. See text for details.

Table 1. Comparison of Calculated and Observed Mass Values of G*n*-OH and G*n*-OH/Cu^{2+} Composites

	obsd mass (Da)[a]	calcd mass (Da)[a]	error (ppm)
G2-OH			
$[M+H]^+$	3273.05	3272.99	18
	3271.06[b]	3271.04[c]	6
$[M+Cu]^+$	3335.78	3335.52	78
	3333.02[b]	3332.97[c]	15
$[M+2Cu-H]^+$	3398.29	3398.06	68
	3394.95[b]	3394.89[c]	18
G3-OH			
$[M+H]^+$	6941.8	6941.45	50
$[M+Cu]^+$	(7004)[d]	7003.99	
$[M+2Cu-H]^+$	(7067)[d]	7066.53	
G4-OH			
$[M+H]^+$	14277.5	14278.38	62
$[M+16Cu-15H]^+$		15278.99	

[a] Values refer to average masses unless specified otherwise. [b] Observed monoisotopic mass obtained from reflectron mode. [c] Calculated monoisotopic mass. [d] Peak centroid is not well-defined.

marized in Table 1. The highest *m*/*z* ion observed in the high-resolution spectrum of G2-OH (inset of Figure 1a) corresponds to the protonated molecule of the ideal (defect-free) structure (M_{IS}, 3271.06). Additional signals are observed at *m*/*z* values less than M_{IS} in integral units of 115 Da [$M_{IS} - x115$]. These signals could be due to fragmentation of the protonated G2-OH ions, e.g., loss of 115 mass units, or the presence of "missing arm" ($-CH_2CH_2CONHCH_2CH_2OH$) defects inside hydroxyl-terminated dendrimers (Scheme 2). The observation of a peak of $M_{IS} - 4 \times 115 - 60$ in the spectrum is assigned to formation of an intramolecular loop during the amidation reaction in the proceeding G1 dendrimer synthesis (M_{IS} − 4 arms + 1 loop) (Scheme 2). The evidence for such signals arising from inherent defects in the dendrimers rather than fragmentation of the gas-phase ion is that the relative abundances for each ion series are not a function of the laser power. The linear TOF mass spectrum of G2-OH is also dominated by the M_{IS} peak and contains ions of the type $M_{IS} - xR$ and $M_{IS} - 4R + 1L$ structures (Scheme 2 and Figure 2a). The observed average M_{IS}, 3273.05, is very close to the calculated value, 3272.99 (Table 1).

Scheme 2

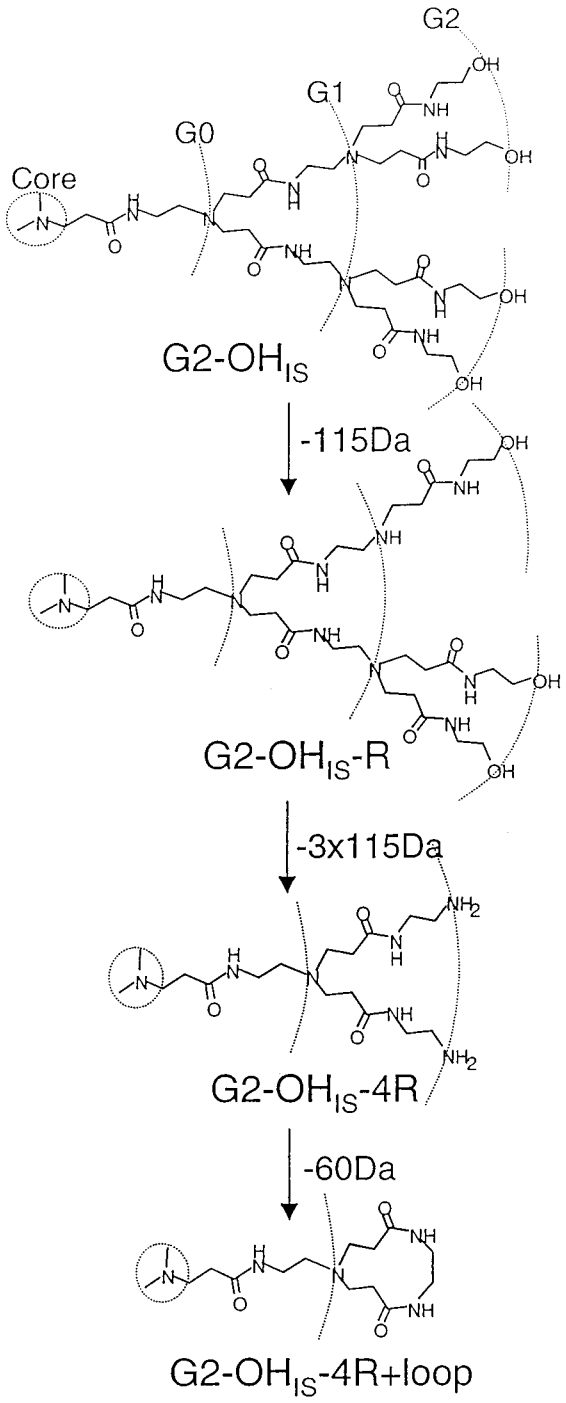

"Missing-arm" defects in dendrimers are a natural consequence of the divergent synthetic strategy, which involves multiple synthetic steps proceeding outward from a central core.[56] Specifically, synthesis of PAMAM dendrimers consists of a reiterative sequence of two basic reactions: a Michael addition of methyl acrylate (MA) to the amine-terminated dendrimer branches and amidation of the resulting methyl ester derivatives with ethylenediamine (EDA) to regenerate the terminal amines. The hydroxyl-terminated dendrimers used in this study were prepared using this approach, except ethanol amine was used for the last amidation step rather than EDA. The "missing arm" defects result from subquantitative success of the Michael reaction. The "missing arm + loop" defects of G2-OH are due to defect propagation from the G1-NH_2 stage. These results

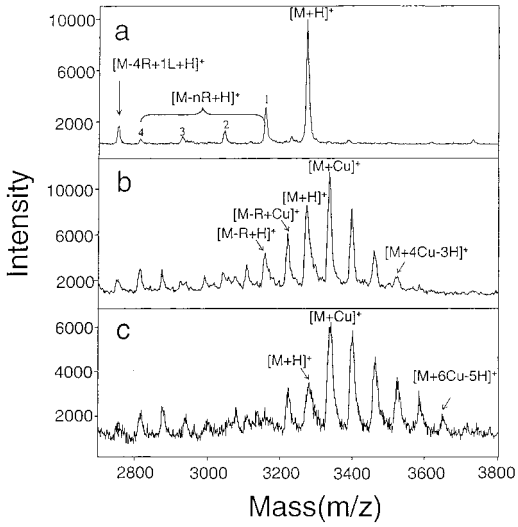

Figure 2. MALDI-linear TOF mass spectra of G2-OH in the (a) absence and presence of a (b) 4-fold and (c) 16-fold molar excess of Cu^{2+}. Matrix: umbelliferone. Notation for peak assignment is the same as in Figure 1.

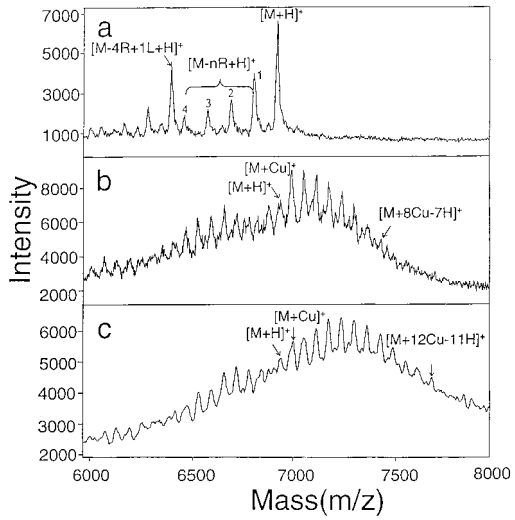

Figure 3. MALDI-linear TOF mass spectra of G3-OH in the (a) absence and presence of an (b) 8-fold and (c) 32-fold molar excess of Cu^{2+}. Matrix: THAP. Notation for the peak assignments is the same as in Figure 1.

suggest that even at low generation, dendrimers start to accumulate defects. The dendrimer molecules with defects (Figures 1a and 2a) have also been observed by electrospray ionization of amine-terminated PAMAM dendrimers.[29] As mentioned earlier, this strongly suggests that the defects are inherent to the synthetic strategy used to prepare the dendrimers rather than being caused by the ionization mechanism.[28,29,34] Interestingly, spectra of amine-terminated dendrimers show defects of M_{IS} + loop, while hydroxyl-terminated dendrimers contain no such defects. This is because the last reactant used to prepare G*n*-OH is hydroxyl-functionalized and thus not able to undergo the chemistry required for loop formation. Accordingly, hydroxyl-terminated PAMAM dendrimers contain less defects than the equivalent amine-terminated materials.

The mass spectrum of G3-OH is very similar to that of G2-OH (Figure 3a). It contains a strong signal at *m*/*z* 6941.8 which corresponds to protonated M_{IS}. The spectrum also contains signals for missing arm and missing arm + loop defects. Interestingly, M_{IS} − 4R + 1L is the

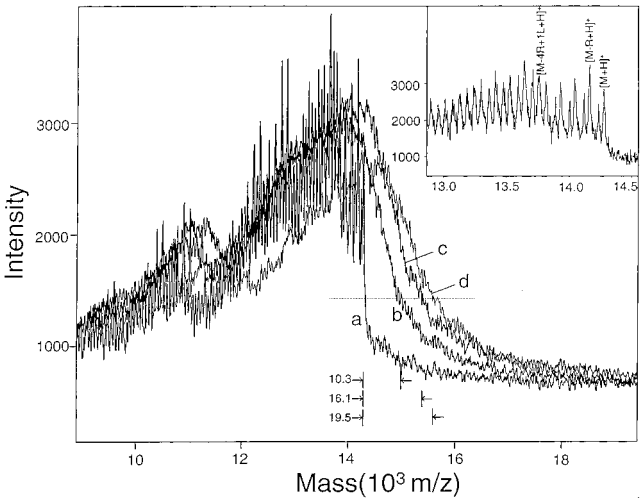

Figure 4. Overlaid MALDI-linear TOF mass spectra of (a) G4-OH only and samples prepared by mixing Cu^{2+} with G4-OH at molar ratios of (b) 10, (c) 16, and (d) 32. Matrix: THAP. The difference in mass between that at half the maximum height of the G4-OH (ideal structure) peak and the other three curves is used to estimate the Cu^{2+} dendrimer loading as a function of the Cu^{2+}/G4-OH ratio (10.3, 16.1, and 19.5 Cu^{2+}/dendrimer for spectra b, c, and d, respectively). The inset shows the expanded spectrum of G4-OH in the region of highest mass. The notation used for peak assignment is the same as Figure 1.

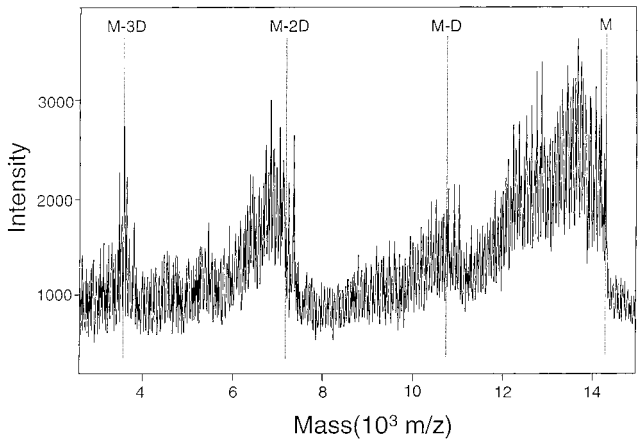

Figure 5. MALDI-TOF mass spectra of G4-OH reveal four distinguishable mass regions. Dashed lines indicate the positions of G4-OH (M) and G4-OH missing one dendron (M-D), two dendrons (M-2D), and three dendrons (M-3D). Matrix: THAP.

most significant defect for G3-OH. This result suggests that loop formation in the higher generation dendrimer is more serious than for lower generation dendrimers.

Mass spectra of G4-OH (Figures 4 and 5) are much more complicated than the previous examples. Although spectrum a in Figure 4 contains a large number of signals, the expanded view (inset) shows individual signals that can be assigned to protonated G4-OH (M_{IS} = 14 277.5) and a series of ions corresponding to missing arm or missing arm + loop dendrimers. Compared to G2-OH and G3-OH, the signals for lower masses become more prominent, and their abundances are even greater than the parent ion. Although in this case the ion abundances vary with laser power, the relative abundances for each ion series are constant, suggesting that the signals for lower mass ions are due to structural defects as opposed to fragmentation of gas-phase ions. Because defects propagate through the divergent syn-

thesis, higher generation dendrimers are expected to contain more defects.[1] Interestingly, the mass spectrum of G4-OH (Figure 5) shows four distinct mass regions, which correspond to G4-OH and G4-OH missing one, two, or three dendrons. In contrast, HPLC data provided by the manufacturer (Dendritech, Inc., Midland, MI) for the G4-OH dendrimers reveal a single peak, suggesting that the concentration of defective structures is small. We cannot rule out the possibility that the ions corresponding to G4-OH missing one, two, or three dendrons are formed by gas-phase fragmentation processes; however, the relative abundances of the defective ions are independent of the laser power used for ionization.

Mass spectra have been used to determine the polydispersity index of polymers.[29,31,57] Polydispersity is characterized by the ratio of the weight-average (M_w) to the number-average molecular weight (M_n). There are two assumptions associated with using MS to calculate polydispersities. First, all the peaks due to loss of R groups and loop formation are only attributable to structural defects generated during synthesis. Significant contributions from fragmentation overestimate the calculated polydispersity. Second, in each sample the ideal and defective dendrimer structures are ionized with equal efficiency; this assumption is well-justified given the chemical similarity between these species. Within the context of these assumptions, the ion abundance for each compound is quantitatively representative of the relative concentration of corresponding species in that sample. The ratio M_w/M_n is calculated to be 1.004, 1.002, and 1.003 for G2-OH, G3-OH, and G4-OH metal-ion free dendrimers, respectively. Even though dendrimers have many defects, these results clearly indicate that they still show near monodispersity compared with other kind of polymers.[31,57]

Cu^{2+}-Containing Dendrimers. We have previously shown that dendrimers, including G4-OH, extract transition-metal ions from solution into their interiors.[9−11,18,20] This finding is expanded upon here to show that MALDI-TOF MS can be used to quantitatively analyze the number of metal ions per dendrimer.

Prior to initiating the MS study, we examined complexation between PAMAM dendrimers and Cu^{2+} in aqueous solutions using UV−vis spectroscopy.[18] Figure 6a shows absorption spectra of 0.8 mM Cu^{2+} in the presence and absence of G4-OH dendrimers. In the absence of G4-OH, Cu^{2+} exists primarily as $[Cu(H_2O)_6]^{2+}$. This complex gives rise to a broad, weak absorption band centered at 810 nm, which arises from the d−d transition of Cu^{2+} in a tetragonally distorted octahedral or square-planar H_2O-ligand field. In the presence of 0.05 mM hydroxyl-terminated PAMAM dendrimers (G*n*-OH, n = 2, 3, and 4), λ_{max} for the d−d transition shifts to 605 nm ($\epsilon \sim 100$ M^{-1} cm^{-1}). In addition, a strong ligand-to-metal charge-transfer (LMCT) transition is centered at 300 nm ($\epsilon \sim 4000$ M^{-1} cm^{-1}).

These data show that Cu^{2+} partitions into the dendrimer from the aqueous phase and that the ligands responsible for binding Cu^{2+} within G*n*-OH are the interior tertiary amines. Evidence for this latter contention comes from the pH dependence of the two absorption bands. For example, both absorption bands decrease in magnitude as the pH is lowered until they finally disappear at pH 3.0. (The spectrum of 0.05 mM G*n*-OH + 0.8 mM Cu^{2+} at pH < 3 is identical to spectrum 2 in Figure 6a.) This result is a consequence of tertiary amine protonation (pK_a = 5.5)[58] and concomitant expulsion of Cu^{2+} at low pH.[18,59,60]

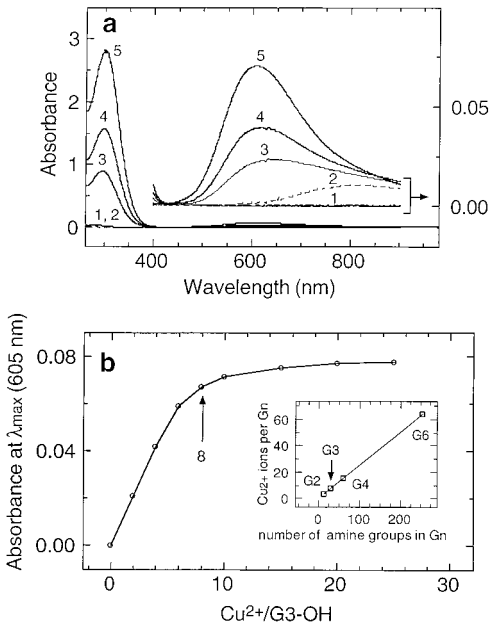

Figure 6. (a) Absorption spectra of 0.8 mM $CuSO_4$ in the presence (spectrum 3, G2-OH; spectrum 4, G3-OH; and spectrum 5, G4-OH) and absence (dashed line, spectrum 2) of 0.05 mM G*n*-OH. Spectrum 1 is the absorption spectrum of 0.05 mM G3-OH vs water. (b) Spectrophotometric titration plot of the absorbance at the peak maximum of 605 nm (part a) as a function of the number of Cu^{2+} ions per G3-OH. The initial concentration of G3-OH was 0.1 mM. The titration end point is estimated as the extrapolated intersection of the two straight lines before and after the equivalence point. The inset shows the relationship between the number of Cu^{2+} ions complexed within G*n*-OH and the number of tertiary amine groups within G*n*-OH. The optical path length was 1 cm.

Figure 6a also shows the effect of dendrimer generation on the absorption spectrum. Specifically, the bands at 605 and 300 nm increase with increasing generation when the dendrimer concentration is held constant at 0.05 mM. This concentration corresponds to a 16/1 Cu^{2+}/G*n*-OH ratio, which is stoichiometric for G4-OH but in excess for the lower generation dendrimers. Accordingly, the absorbance in the higher generation dendrimers increases because of increased intradendrimer Cu^{2+}.

To learn more about the Cu^{2+} ligand field, we quantitatively analyzed the number of Cu^{2+} ions extracted into each dendrimer by spectrophotometric titration. These data confirm and expand upon results previously reported.[18] For example, Figure 6b is a plot of absorbance at the peak maximum of 605 nm against the Cu^{2+}/dendrimer ratio for G3-OH. Lines extrapolated from the two linear regions of this curve intersect at a Cu^{2+}/dendrimer ratio of 8, indicating that each G3-OH can strongly bind eight Cu^{2+} ions. Additional spectrophotometric titrations indicate that G2-OH, G4-OH, and G6-OH strongly sorb a maximum of 4, 16, and 64 Cu^{2+} ions, respectively (Figure 6b, inset).

Mass spectral data also provide information about the number of metal ions complexed to dendrimers. For example, a solution of G2-OH mixed with a 4-fold molar excess of Cu^{2+} results in the MS spectra shown in Figures 1b and 2b. Figure 1b indicates that Cu^{2+} complexes with ideal-structure dendrimers, as well as to dendrimers containing defects, but that the former are most prominent. The spectrum also exhibits well-resolved isotopic multiplets of the $[M_{IS} + Cu(I)]^+$ ion (inset of Figure 1b). Moreover, there is good agreement

between the measured and theoretical isotopic patterns. Importantly, Figure 2b confirms a key element of the UV−vis spectroscopic data described earlier; that is, G2-OH sorbs up to four Cu^{2+} ions.

The oxidation state of copper ions complexed to G2-OH after desorption/ionization in the mass spectrometer can be established using accurate mass measurements. The mass differences between the monoisotopic peaks of the protonated dendrimer and the single- and double-copper adducts are 61.96 and 61.93, which is consistent with the assignment of the adduct ions as $[M_{IS} + Cu(I)]^+$ and $[M_{IS} + 2Cu(I)\text{-}H]^+$ (Figure 1b). Moreover, the separation between adjacent copper adducts in Figure 2b is ~62.5, which is also consistent with the aforementioned assignments. We speculate that these results arise from Cu^{2+} being reduced photochemically to Cu^+ during the laser ionization process.[37,61] This effect has been observed previously in MALDI MS when polymers[62] or peptides[63,64] were used as copper ligands.

The relative abundances of the four copper adducts do not necessarily reflect the absolute concentrations of the individual species in the sample. Because addition of each copper to the dendrimer has to be accompanied by loss of a proton to form the singly charged ion, higher Cu^{2+}-loading species are less favored than lower Cu^{2+}-loading species during the MALDI ionization process.

The UV−vis spectroscopic data indicated that each G2-OH can strongly sorb as many as four Cu^{2+} ions but that an increase in the solution-phase Cu^{2+}/dendrimer ratio results in an increase in the number of Cu^{2+} ions sequestered within the dendrimer.[65] Accordingly, we investigated this effect by mass spectrometry. For example, when the Cu^{2+}/G2-OH ratio is increased to 16, two additional Cu^{2+} adduct peaks are evident in the mass spectrum (Figure 2c). Taken together with the UV−vis spectroscopic data, these results indicate that there are some weak ion-binding sites for Cu^{2+} within the dendrimers.

Similar results are obtained when G3-OH is exposed to an excess of Cu^{2+}. As shown in Figure 6b, the spectroscopic data indicate eight strong binding sites in G3-OH, and the corresponding mass spectrum (Figure 3b) shows dendrimer adducts containing up to eight Cu^{2+} ions. However, when the Cu^{2+}/G3-OH ratio is increased to 32, a maximum of 12 Cu^{2+} ions is observed in the mass spectrum (Figure 3c). As for G2-OH, we believe that these extra ions occupy weak binding sites within the dendrimer, which is why only a slight increase is observed in the UV−vis absorbance intensity after the first eight Cu^{2+} ions are sequestered within the dendrimer.[65]

Spectrum a of Figure 4 shows the mass spectrum of G4-OH without added Cu^{2+}, while spectra b−d contain 10, 16, and 32-fold molar excesses of Cu^{2+}, respectively. The *m*/*z* envelope shifts to higher values as the amount of Cu^{2+} increases, but the overall appearance of the spectra changes very little. For example, the fine structure shown in the inset of Figure 4 is still partially resolved. However, the slopes of the curves for spectra b−d indicate some tailing at higher *m*/*z* ratios, which we speculate could indicate attachment of weakly bound Cu^{2+} to G4-OH or that some of the dendrimer−Cu^{2+}-adduct ions strongly absorb at 337 nm (the laser wavelength; see Figure 6a) and undergo photodissociation.

Summary and Conclusions

MALDI-TOF is an efficient method for analyzing PAMAM dendrimers and their complexes with Cu^{2+}. For PAMAM dendrimers up to generation 4 and masses up to 14 kDa, parent ions and ions due to structural defects are observed with high resolution and mass accuracy. MALDI-TOF also confirms UV−vis titrations, which indicate that the number of Cu^{2+} ions that can be strongly bound within a particular generation dendrimer scales as half the number tertiary amines in the outer dendritic shell. The MS data also show that when the molar excess of Cu^{2+} is increased, additional ions enter the dendrimer where they reside in weaker binding sites. MALDI-TOF data of the type described here should be valuable for studying other host−guest interactions between dendrimers and metal ions, metal and semiconductor nanoparticles,[66] small molecules, and perhaps complexes between dendrimers and biomolecules such as DNA.

Acknowledgment. This work was supported by the National Science Foundation (R.M.C., CHE-9818302) and the U.S. Department of Energy, Division of Chemical Science, OBES (D.H.R.). Additional support to R.M.C. was provided via subcontract from Sandia National laboratories, which is supported by the U.S. Department of Energy (Contract DE-AC04-94AL8500). Sandia is a multiprogram laboratory operated by the Sandia Corporation, a Lockheed-Martin company, for the U.S. Department of Energy. M.Z. acknowledges fellowship support from The Electrochemical Society, Inc., the Eastman Chemical Company, and Phillips Petroleum. We also thank Mr. Mark Kaiser (Dendritech, Inc., Midland, MI) for helpful discussions and for providing the Starburst PAMAM dendrimers used in this study.

References and Notes

(1) Zeng, F.; Zimmerman, S. C. *Chem. Rev.* **1997**, *97*, 1681−1712.
(2) Fischer, M.; Vögtle, F. *Angew. Chem., Int. Ed. Engl.* **1999**, *38*, 884−905.
(3) Tomalia, D. A.; Kaplan, D. A.; Kruper, W. J., Jr.; Cheng, R. C.; Tomlinson, I. A.; Fazio, M. J.; Edwards, D. S. US Patent 5 728 461, 1994.
(4) Newkome, G. R.; Moorefield, C. N.; Keith, J. M.; Baker, G. R.; Escamilla, G. H. *Angew. Chem., Int. Ed. Engl.* **1994**, *33*, 666−668.
(5) Armspach, D.; Cattalini, M.; Constable, E. C.; Housecroft, C. E.; Phillips, D. *J. Chem. Soc., Chem. Commun.* **1996**, 1823−1824.
(6) Wells, M.; Crooks, R. M. *J. Am. Chem. Soc.* **1996**, *118*, 3988−3989.
(7) Tokuhisa, H.; Crooks, R. M. *Langmuir* **1997**, *13*, 5608.
(8) Knapen, J. W. J.; can der Made, A. W.; de Wilde, J. C.; van Leeuwen, P. W. N. M.; Wijkens, P.; Grove, D. M.; van Koten, G. *Nature* **1994**, *372*, 659−663.
(9) Zhao, M.; Crooks, R. M. *Adv. Mater.* **1999**, *11*, 217−220.
(10) Zhao, M.; Crooks, R. M. *Angew. Chem., Int. Ed. Engl.* **1999**, *38*, 364−366.
(11) Chechik, V.; Zhao, M.; Crooks, R. M. *J. Am. Chem. Soc.* **1999**, *121*, 4910−4911.
(12) Bourque, S. C.; Maltais, F.; Xiao, W.-J.; Tardif, O.; Alper, H.; Arya, P.; Manzer, L. E. *J. Am.Chem. Soc.* **1999**, *121*, 3035−3038.
(13) Jansen, J. F. G. A.; de Brabander-van den Berg, E. M. M.; Meijer, E. W. *Science* **1994**, *266*, 1226−1229.
(14) Ottaviani, M. F.; Bossmann, S.; Turro, N. J.; Tomalia, D. A. *J. Am. Chem. Soc.* **1994**, *116*, 661−671.
(15) Ottaviani, M. F.; Turro, C.; Turro, N. J.; Bossmann, S. H.; Tomalia, D. A. *J. Phys. Chem.* **1996**, *100*, 13667−13674.
(16) Ottaviani, M. F.; Turro, N. J.; Jockusch, S.; Tomalia, D. A. *Colloid Surf. A* **1996**, *115*, 9−21.

(17) Ottaviani, M. F.; Turro, N. J.; Jockusch, S.; Tomalia, D. A. *J. Phys. Chem.* **1996**, *100*, 13675−13686.
(18) Zhao, M.; Sun, L.; Crooks, R. M. *J. Am. Chem. Soc.* **1998**, *120*, 4877−4878.
(19) Matthews, O. A.; Shipway, A. N.; Stoddart, J. F. *Prog. Polym. Sci.* **1998**, *23*, 1−56.
(20) Chechik, V.; Crooks, R. M. *J. Am. Chem. Soc.* **2000**, *122*, 1243−1244.
(21) Valden, M.; Lai, X.; Goodman, D. W. *Science* **1998**, *281*, 1647−1650.
(22) Brousseau, L. C.; Zhao, Q.; Shultz, D. A.; Feldheim, D. L. *J. Am. Chem. Soc.* **1998**, *120*, 7645−7646.
(23) Grabar, K. C.; Brown, K. R.; Keating, C. D.; Stranick, S. J.; Tang, S.-L.; Natan, M. J. *Anal. Chem.* **1997**, *69*, 471−477.
(24) Mirkin, C. A.; Letsinger, R. L.; Mucic, R. C.; Storhoff, J. J. *Nature* **1996**, *382*, 607−609.
(25) Striegel, A. M.; Plattner, R. D.; Willett, J. L. *Anal. Chem.* **1999**, *71*, 978−986.
(26) Brothers, H. M.; Piehler, L. T.; Tomalia, D. A. *J. Chromatogr. A* **1998**, *814*, 233−246.
(27) Hobson, L. J.; Feast, W. J. *Polymer* **1999**, *40*, 1279−1297.
(28) Schwartz, B. L.; Rockwood, A. L.; Smith, R. D.; Tomalia, D. A.; Spindler, R. *Rapid Commun. Mass Spectrom.* **1995**, *9*, 1552−1555.
(29) Kallos, G. J.; Tomalia, D. A.; Hedstrand, D. M.; Lewis, S.; Zhou, J. *Rapid Commun. Mass Spectrom.* **1991**, *5*, 383−386.
(30) Weener, J.-W.; van Dongen, J. L. J.; Meijer, E. W. *J. Am. Chem. Soc.* **1999**, *121*, 10346−10355.
(31) Hummelen, J. C.; van Dongen, J. L. J.; Meijer, E. W. *Chem. Eur. J.* **1997**, *3*, 1489−1493.
(32) van der Wal, S.; Mengerink, Y.; Brackman, J. C.; de Brabander, E. M. M.; Jeronimus-Stratingh, C. M.; Bruins, A. P. *J. Chromatogr. A* **1998**, *825*, 135−147.
(33) Pesak, D. J.; Moore, J. S.; Wheat, T. E. *Macromolecules* **1997**, *30*, 6467−6482.
(34) Tolic, L. P.; Anderson, G. A.; Smith, R. D.; Brothers, H. M., II; Spindler, R.; Tomalia, D. A. *Int. J. Mass Spectrom. Ion. Processes* **1997**, *165/166*, 405−418.
(35) Russell, D. H.; Edmondson, R. D. *J. Mass Spectrom.* **1997**, *32*, 263−276.
(36) Hillenkamp, F. K. M. *Anal. Chem.* **1991**, *63*, 1193A−1203A.
(37) (a) Wong, C. K. L.; Chan, T.-W. D. *Rapid Commun. Mass Spectrom.* **1997**, *11*, 513−519. (b) Mallis, L. M.; Russell, D. H. *J. Mass Spectrom. Ion Processes* **1987**, *78*, 147−148.
(38) Leon, J. W.; Fréchet, J. M. J. *Polym. Bull.* **1995**, *35*, 449−455.
(39) Wendland, M. S.; Zimmerman, S. C. *J. Am. Chem. Soc.* **1999**, *121*, 1389−1390.
(40) Chessa, G.; Scrivanti, A.; Seraglia, R.; Traldi, P. *Rapid Commun. Mass Spectrom.* **1998**, *12*, 1533−1537.
(41) Wu, Z.; Biemann, K. *Int. J. Mass. Spectrom. Ion Processes* **1997**, *165/166*, 349−361.
(42) Kim, C.; Jung, I. *J. Organomet. Chem.* **1999**, *588*, 9−19.
(43) Kawaguchi, T.; Walker, K. L.; Wilkins, C. L.; Moore, L. S. *J. Am. Chem. Soc.* **1995**, *117*, 2159−2165.
(44) Leon, J. W.; Kawa, M.; Fréchet, J. M. J. *J. Am. Chem. Soc.* **1996**, *118*, 8847−8859.
(45) Mowat, I. A.; Donovan, R. J.; Bruce, M.; Feast, W. J.; Stainton, N. M. *Eur. Mass Spectrom.* **1998**, *4*, 451−458.
(46) Seebach, D.; Herrmann, G. F.; Lengweiler, U. D.; Amrein, W. *Helv. Chim. Acta* **1997**, *80*, 989−1026.
(47) Leduc, M. R.; Hayes, W.; Fréchet, J. M. J. *J. Polym. Sci.* **1998**, *36*, 1−10.
(48) Yu, D.; Vladimirov, N.; Fréchet, J. M. J. *Macromolecules* **1999**, *32*, 5186−5192.
(49) Bo, Z.; Zhang, W.; Zhang, X.; Zhang, C.; Shen, J. *Macromol. Chem. Phys.* **1998**, *199*, 1323−1327.
(50) Emran, S. K.; Newkome, G. R.; Weis, C. D.; Harmon, J. P. *J. Polym. Sci.* **1999**, *37*, 2025−2038.
(51) Barbacci, D. C.; Edmondson, R. D.; Russell, D. H. *Int. J. Mass Spectrom.* **1997**, *165*, 221−235.
(52) Koonen, J. M.; Russell, W. K.; Hettick, J. M.; Russell, D. H. *Anal. Chem.* **2000**, *72*, 3860−3866.
(53) For additional discussion of sample preparation of polymers for MALDI analysis, see: Nielen, M. W. F. *Mass Spectrom. Rev.* **1999**, *18*, 309−344.
(54) Montaudo, G.; Garozzo, D.; Montaudo, M. S.; Puglisi, C.; Samperi, F. *Macromolecules* **1995**, *28*, 7983−7989.
(55) Montaudo, G.; Scamporrino, E.; Vitalini, D.; Mineo, P. *Rapid Commun. Mass Spectrom.* **1996**, *10*, 1551−1556.
(56) Tomalia, D. A.; Naylor, A. M.; Goddard, W. A. G., III *Angew. Chem., Int. Ed. Engl.* **1990**, *29*, 138−175.
(57) Zhu, H. H.; Yacin, T.; Li, L. *J. Am. Soc. Mass Spectrom.* **1998**, *9*, 275−281.
(58) Dendritech *Technology Review*, 1995.
(59) Ottaviani, M. F.; Cossu, E.; Turro, N. J.; Tomalia, D. A. *J. Am. Chem. Soc.* **1995**, *117*, 4387−4398.
(60) Niu, Y.; Sun, L.; Crooks, R. M., manuscript in preparation.
(61) Yalcin, T.; Schriemer, D. C.; Li, L. *J. Am. Soc. Mass Spectrom.* **1997**, *8*, 1220−1229.
(62) Lienes, C. F.; Omalley, R. M. *Rapid Commun. Mass Spectrom.* **1992**, *6*, 564−570.
(63) Bouchonnet, S.; Hoppilliard, Y.; Ohanessian, G. *J. Mass Spectrom.* **1995**, *30*, 172−179.
(64) Shields, S. J.; Bluhm, B. K.; Russell, D. H. *Int. J. Mass Spectrom.* **1999**, *183*, 185−195.
(65) The pH of the solutions used to obtain the data in Figure 6 was not controlled because buffers interfere with the dendrimer/Cu^{2+} binding equilibrium. For example, the titration of G4-OH began at ~pH 8 and ended at ~pH 5 (a consequence of the addition of Cu^{2+} to the solution). This change in pH affects titration plots such as the one shown in Figure 6b, because H^+ competes more effectively with Cu^{2+} for dendrimer binding sites at low pH (toward the end of the titration). As a consequence, the slope of the linear portion of the plot at high Cu^{2+}/dendrimer ratios is slightly reduced from its true value. This artifact does not significantly affect the measured end points. A full description of the complicated behavior of Cu^{2+}/dendrimer solutions as a function of pH will be forthcoming (see ref 60).
(66) Lemon, B. I.; Crooks, R. M. *J. Am. Chem. Soc.* **2000**, *122*, 12886−12887.

MA001782J